

## Ab-initio Calculation of Electronic Structures and Magnetic Properties of Dilute Aluminium Pnictides

Mohammad Shahjahan,<sup>1,2</sup> Tanjila Khan,<sup>1,2</sup> Md. Forman Ullah<sup>1,2</sup> and  
Mohammad Mizanur Rahman<sup>2\*</sup>

<sup>1</sup>Center for Advanced Research in Sciences, University of Dhaka,  
Dhaka-1000, Bangladesh

<sup>2</sup>Department of Physics, University of Dhaka, Dhaka-1000, Bangladesh

\*Corresponding author: mmizan@du.ac.bd

Published online: 25 November 2019

To cite this article: Shahjahan, M. et al. (2019). Ab-initio calculation of electronic structures and magnetic properties of dilute aluminium pnictides. *J. Phys. Sci.*, 30(3), 11–20, <https://doi.org/10.21315/jps2019.30.3.2>

To link to this article: <https://doi.org/10.21315/jps2019.30.3.2>

**ABSTRACT:** *Electronic structures and magnetic properties of dilute aluminium pnictides ( $Al_{1-x}T_xM$ ) are calculated on the basis of density functional theory, where  $T$  denotes 3d transition metal (TM) elements and  $M$  denotes As and P elements. Among the TM elements, V, Cr, Fe and Co are used as dopants, which are used sequentially at the cation sites of the pnictide semiconductors. Ferromagnetic (FM) critical temperature ( $T_c$ ) is calculated using the mean-field approximation combined with the Korringa-Kohn-Rostoker Green's function method. Self-consistent energy minimisation scheme is used to select the stable magnetic state as well as the calculation of  $T_c$  between the FM state and disordered local moment (DLM) state. Furthermore, electronic structures are calculated for the stable magnetic states of these compounds. A significant change in  $T_c$  is obtained for varying doping concentrations. Saturated magnetisations of those stable compounds are consistent with the variation of doping concentrations, whereas spin magnetisations are found to be nearly independent of doping concentrations.*

**Keywords:** KKR-Green's function, coherent potential approximation, aluminium pnictides, atomic sphere approximation, density of states

### 1. INTRODUCTION

Dilute magnetic semiconductors (DMS) are an attractive research field for the last few decades for nano-magnetism and nanosize material fabrications.<sup>1</sup> Some of the DMS, namely (Ga, Mn)As, (Ga, Mn)N, (Zn, Cr)O and (Zn, Cr)Te are considered

promising spintronic materials.<sup>2,3</sup> They exhibit various magnetic features, which are governed by different kinds of exchange interactions such as Zener's double-exchange, Zener's p-d exchange and super-exchange mechanisms.<sup>4-8</sup> Although the magnetic states and magnetic properties can be calculated by ab-initio methods, the physical understanding of the involved exchange interactions is a very intuitive problem, such that a multitude of mechanisms can lead to ferromagnetism or antiferromagnetism and often some of them may act simultaneously.

The electronic devices have made revolutionary change over the past few decades after the invention of integrated circuit (IC). The advantages of integration will bring a proliferation and reliability of electronics. More sophisticated IC is needed for improving performance of electronic devices and profitability in the microelectronics industry. Technologically, it is difficult to further scaling down the IC size. Required excessive high power is the main impediment for further reducing the IC size. Therefore, newer approaches have constantly been investigated in order to miniaturisation of microelectronics.<sup>9</sup> One of the attempts is the spintronic devices.

Spintronics means spin-based electronics.<sup>10</sup> It is a modern branch of electronics emerged from the DMS. Main aspect of spintronics is the utilisation of electronic spin in addition to the charge of the carrier in transition metal (TM) doped semiconductors. At present, electronic devices function with controlling charge transfer ignoring the spin of electrons. The manipulation of the spin of electrons along with charge open up faster and more efficient devices for quantum computation. Other advantage of spintronics is that it needs relatively low energy to manipulate the orientation of spin of an electron, which could allow to develop devices with less energy consumption capability.

Magnetic materials with spintronic property have various applications in our daily life. For example, hard drives, magnetoresistive random-access memory (MRAM), spin transistor and read-write heads are widely used in the practical purposes. On the other hand, new functionalities can be induced in semiconductor spintronic devices. The focal points of semiconductor spintronics are doping, manipulation, transfer and detection of spin polarised carriers. In the present calculation, substitutional doping of magnetic atoms is manipulated with coherent potential approximation (CPA).<sup>11</sup> A ferromagnetic (FM) element is required for generating spin polarised carriers in the semiconductors. The FM materials have unequal density of states (DOS) at the Fermi level, whereas disordered local moment (DLM) state exhibits equal DOS at the Fermi level for majority and minority carriers. These FM materials offer a high degree of spin polarisation at the Fermi level.<sup>12</sup>

Usually, some DMS exhibit FM critical temperature ( $T_C$ ) lower than the room temperature (RT). However, these types of DMS are not compatible with the requirements of the existing technology. Therefore, the main objective of the present research is to find DMS, which can exhibit  $T_C$  higher than RT. At present, it is the most challenging task to predict DMS with high  $T_C$ , because the underlying mechanism of their ferromagnetism has not been clearly understood yet. Recently, Dietl et al. proposed a model called Zener's p-d exchange model to describe the carrier induced ferromagnetism and predicted some DMS with high  $T_C$ . This calculation was carried out considering mean field approximation (MFA).<sup>13,14</sup> In this article, we present electronic structures, Curie temperature,  $T_C$  and magnetic properties of TM doped zincblende type compounds with chemical formula  $(Al_{1-x}T_x)M$ , where T represents V, Cr, Fe, and Co and M denotes As and P. The DOS is calculated to explain the various FM properties induced in the DMS systems.

## 2. METHODS OF CALCULATION

The self-consistent Korringa-Kohn-Rostoker (KKR) Green's function method is used to calculate the electronic structures of the TM doped aluminium pnictides.<sup>15–17</sup> Generalised gradient approximation (GGA) is used for exchange-correlation energy functional in the calculation.<sup>18</sup> The shape of the potentials are considered as Muffin tin (MT) potential approximation and atomic sphere approximation (ASA). The MT potential is considered to be spherically symmetric inside the atomic sphere and constant in the interstitial regions. In ASA technique, the atomic spheres are considered partially overlapped to each other and in MT potential, spheres just touch each other. The accuracy of ASA potential is deemed better than MT potential and it reproduces the bulk properties of periodic systems very well. In the present case, the TM impurities are introduced randomly into the cation sites of the host semiconductors. This substitutional disordered system is well described by the CPA method.<sup>11</sup> In CPA, average electronic properties are considered instead of properties of respective doping element. The electronic wave functions are calculated here for the angular momentum quantum number defined at each atomic site up to  $\ell = 2$  and  $\ell = 0$  for  $d$  and  $s$  electrons, respectively. Irreducible part of the first Brillouin zone is sampled with 256K sampling points. For convenience of the calculation, we have considered the fixed lattice constants of 5.66 Å and 5.45 Å of the host crystal structures AlAs and AlP, respectively in the TM doped compound structures.<sup>19,20</sup> In the present calculation, we have used the KKR-CPA programme package "Machikaneyama" developed by Akai.<sup>21</sup>

### 3. RESULTS AND DISCUSSION

#### 3.1 Magnetic Properties of Aluminium Pnictide Type DMS

We have analysed magnetic phase stability,  $T_C$  and electronic structures of group III-V type DMS such as  $(Al_{1-x}T_x)As$ , and  $(Al_{1-x}T_x)P$ .<sup>22</sup> The basic compound semiconductors are doped systematically with 3d TM atoms, namely V, Cr, Fe and Co at the host cation sites. We perform magnetic calculations, where spin degeneracy is taken into account. We obtain two magnetic states such as FM and DLM states. The former state exhibits saturated magnetisation as well as the local spin moments with zero orbital moment. The orbital moment will be nonzero for consideration of spin-orbit coupling interactions. In contrast, the latter state is a null magnetisation state arising for random orientation of the associated spins. We calculate total energy per unit cell for FM and DLM states and find the relatively lower energy state, which is termed the stable state. For stable FM state then we calculate the FM transition temperature, above which the material becomes paramagnetic.

In the case of V and Cr-doped AIAs, FM states are more stable than the corresponding DLM states. Phase transition from the FM state to the DLM state occurs at the Curie point in AIAs and AIP based DMS. In the case of Fe and Co doping compounds, negative energy differences are found, which is shown in Table 1 and Table 2 for both the pnictide compounds. In Fe and Co doping cases, the total energy of FM state is higher than that of the DLM state. In these two cases, the lower energy situation is found for DLM state only. Therefore, DLM state is relatively lower in total energy consideration compared with the FM state in the Fe and Co doping cases.

Along with the energy difference, net and local magnetic moments with  $T_C$  are also tabulated in the tables. The bracketed  $T_C$  values are calculated with MT potential approximation, whereas the rest of the data are calculated using ASA potential. An important feature is observed that the energy difference for 10% TM doped case is higher than that of 5% TM doped case and this trend is consistent with the prediction given by Dietl et al.<sup>3</sup> Figures 1(a and b) show the energy differences  $\Delta E$  between DLM and FM states versus V concentrations in the host AIAs and AIP compounds, respectively. The graphical pattern is parabolic in shape and it is found that the  $\Delta E$  gradually increases with increasing doping concentrations. In principle, the threshold value of concentration indicates some phase changes such as if  $\Delta E$  becomes zero then the doped material can be non-magnetic metallic, and for some typical concentrations if  $\Delta E$  becomes positive then the doped material is ferromagnetic, whereas, for negative  $\Delta E$  the material is paramagnetic with a dominating DLM state.

Table 1: Net magnetic moment per unit cell and local spin moment per atom in the FM state of  $(Al_{1-x}T_x)As$  and the corresponding energy difference between FM and DLM states for different TM atoms. The bracketed values of  $T_C$  shown in the last column are calculated using the MT potential approximation.

Materials $(Al_{1-x}T_x)M$	Net moment ( $\mu_B/\text{cell}$ )	Spin moment ( $\mu_B/\text{atom}$ )	$\Delta E$ (mRy)	$T_C$ (K)
$(Al_{0.90}V_{0.10})As$	0.20	1.97	0.156	164 (344)
$(Al_{0.90}Cr_{0.10})As$	0.30	3.05	0.637	670 (686)
$(Al_{0.90}Fe_{0.10})As$	0.42	3.34	-0.669	–
$(Al_{0.90}Co_{0.10})As$	0.20	1.69	-0.079	–

Table 2: Net magnetic moment per unit cell and local spin moment per atom in the FM state of  $(Al_{1-x}T_x)P$  and the corresponding energy difference between the FM and DLM states for different TM atoms. The bracketed values of  $T_C$  shown in the last column are calculated using MT potential approximation.

Materials $(Al_{1-x}T_x)P$	Net moment ( $\mu_B/\text{cell}$ )	Spin moment ( $\mu_B/\text{atom}$ )	$\Delta E$ (mRy)	$T_C$ (K)
$(Al_{0.90}V_{0.10})P$	0.19	1.78	0.556	585 (429)
$(Al_{0.90}Cr_{0.10})P$	0.30	3.03	0.905	953 (772)
$(Al_{0.90}Fe_{0.10})P$	0.49	4.68	-1.069	–
$(Al_{0.90}Co_{0.10})P$	0.39	3.74	-1.353	–

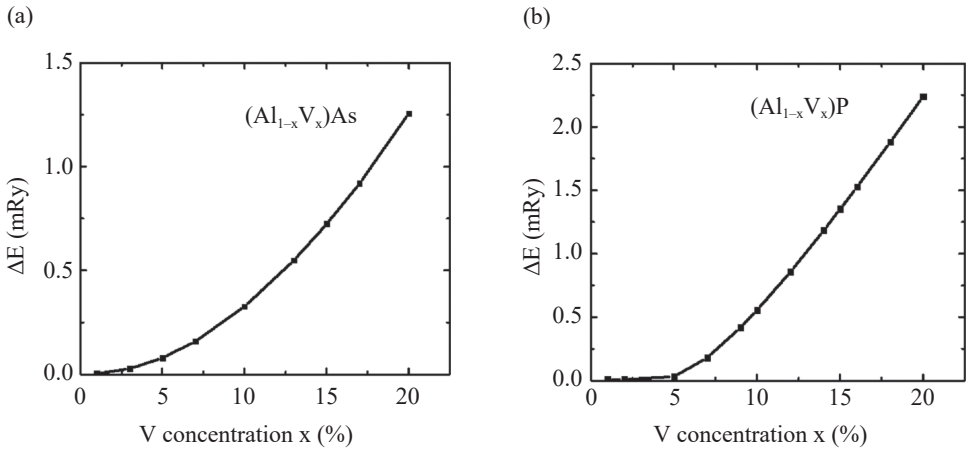


Figure 1: Energy difference  $\Delta E$  in mRy per unit cell vs. doping of V concentrations at the range of 0% (nonmagnetic) to 20% in the host (a) AlAs, and (b) AlP compounds.

The TM atoms such as V and Cr are doped at the  $Al^{3+}$  sites of the pnictide compounds, which require three electrons to fill up its valence band. In this situation doping elements V and Cr will contribute  $d^2$  and  $d^3$  conduction electrons. Since in Cr doped case, p-d hybridisation is much stronger to be considered for more interacting electrons rather than V doped case, therefore its energy difference as well as  $T_C$  is higher than V doped case. The Cr doped material exhibits  $T_C$  higher than RT and half-metallic behaviour. It is easier to handle for spintronics application at ambient condition. Therefore, Cr doped alloy seems better than other alloys with other TM elements. The calculated  $T_C$  in Kelvin against concentrations of Cr in AlAs and AlP are shown in the Figures 2(a and b), respectively. The dotted horizontal line indicates the RT level. In the lower range of Cr concentrations, the values of  $T_C$  increase rapidly but in the higher range of concentrations increasing rate of  $T_C$  become smaller than the lower region. The calculated  $T_C$  is found to be higher than RT in Figures 2(a and b) with dopant concentrations above 2.5% and 1.5%, respectively.

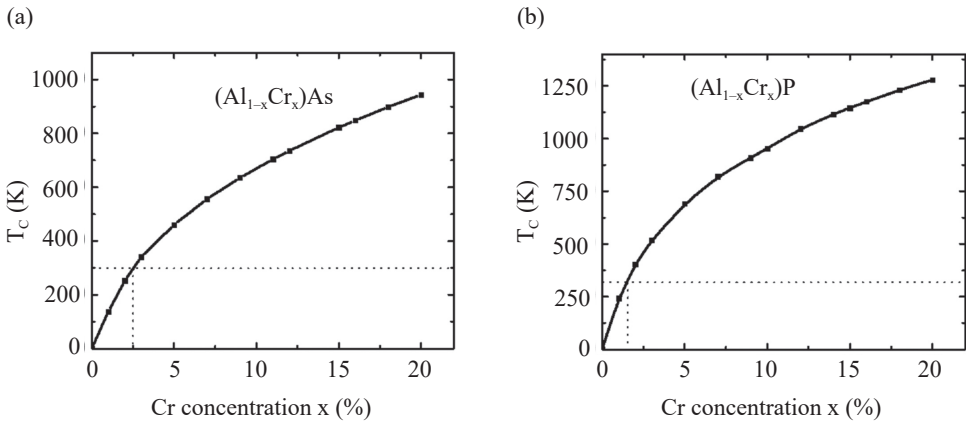


Figure 2: Curie temperature  $T_C$  (in K) against Cr doping concentrations in (a)  $(Al,Cr)As$ , and (b)  $(Al,Cr)P$  at a range of 0% (nonmagnetic) to 20% atomic concentrations.

### 3.2 Calculation of Electronic DOS

The calculated electronic DOS are shown in Figures 3(a and b). From the figures, it is clearly seen that the carriers occupy either localised impurity states or delocalised continuum states in the conduction band or valence band. In the simplest case, each impurity has a single, non-degenerate state. Thus, the density of impurity states corresponds to the concentration of TM atoms. The impurity states mix with the host valence states and often dominate over the total DOS at some ranges of energy. In order to completely understand the origin of ferromagnetism in semiconductors, we have calculated the total DOS and partial DOS of 3d orbital

electrons. The total DOS was evaluated per unit cell and partial DOS are calculated per atomic orbitals. Figure 3(a) shows the total DOS and partial DOS of Al and As p-states of the host AIAs semiconductor. We see that there exists a gap region near the Fermi zone, which indicates the semiconducting nature of AIAs. In Figure 3(b), the vertical axis above and below the zero level represents spin-up and spin down DOS, while the horizontal axis denotes the energy relative to Fermi energy. At the Fermi level, only one spin band has appeared in the semiconducting gap zone and leading to a half metallic nature of the doped compound. The narrow and sharp peaks of the 3d electronic states are straddling around the Fermi level with unequal DOS, giving rise to a net magnetisation. The states beyond the Fermi level are unoccupied, while the states below the Fermi level are fully occupied.

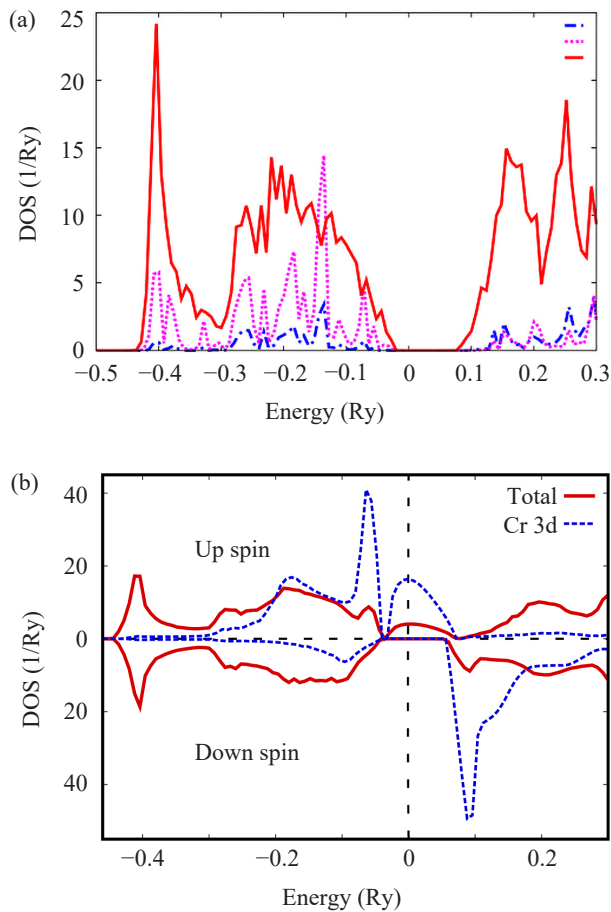


Figure 3: Total and partial DOS of (a) host AIAs semiconductor with p-states of Al and As, and (b)  $(\text{Al}_{0.90}\text{Cr}_{0.10})\text{As}$  magnetic semiconductor with Cr 3d states. The vertical dashed line indicates the Fermi level.

In Figures 4(a and b), total and local DOS of V and Cr doped in AIP are shown, respectively, where up spin d-electron states appear at the Fermi level with no electronic states at the Fermi level for down spin electrons. The narrow and sharp spikes indicate the localised nature of the d-electron DOS compare to the wide and flat s-electron DOS. The impurity states, which are basically anti-bonding states originating from the hybridisation between impurity *d*-electrons and host *s*-electrons of the valence band, appear in the band gap region.<sup>23</sup> The DOS curves confirm that due to V and Cr substitution at the Al site, the compound has a half-metallic character. This behaviour occurs because of the bands near the Fermi level, where majority spins are metallic and minority spins are semiconducting characters.

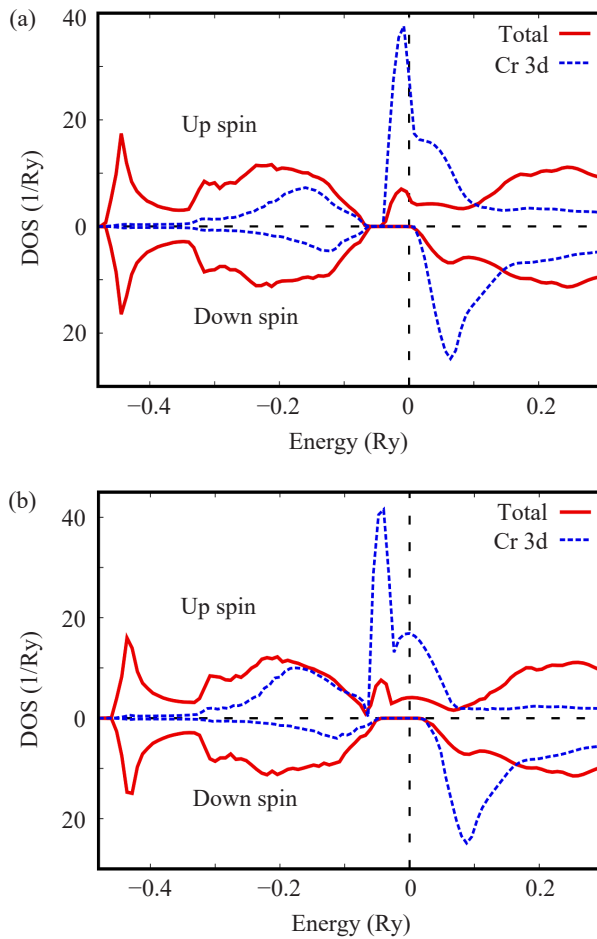


Figure 4: Total and local 3d DOS of (a) V doped  $(\text{Al}_{0.90}\text{V}_{0.10})\text{P}$ , and (b) Cr doped  $(\text{Al}_{0.90}\text{Cr}_{0.10})\text{P}$  magnetic semiconductors.



#### 4. CONCLUSION

We have analysed the magnetic properties, electronic structures and  $T_C$  of dilute aluminium pnictides and obtained FM materials exhibiting  $T_C$  higher than RT. From the numerical calculations, we have found that V and Cr doped AIs and AIP are prospective candidates for high  $T_C$  FM materials, whereas FM state becomes unstable with Fe and Co impurity ions. In some compounds,  $T_C$  increases up to a certain level by increasing doping concentrations. The calculated properties of DMS may explore a research field in the spintronics, where spin-based magnetism plays critical roles. The DOS is calculated to explain the various magnetic states, which are created from the doping of semiconductors. The emerged impurity bands straddle the Fermi level in the band gap area, which are responsible for the ferromagnetism in DMS. This evidence strongly agrees with the Zener's double-exchange model as the origin of ferromagnetism.

#### 5. ACKNOWLEDGEMENTS

The present work was performed using the advanced computing facilities of Centre for Advanced Research in Sciences (CARS), University of Dhaka, Bangladesh.

#### 6. REFERENCES

1. Ohno, H. (1998). Making nonmagnetic semiconductors ferromagnetic. *Sci.*, 281, 951–956, <https://doi.org/10.1126/science.281.5379.951>.
2. Jungwirth, T. et al. (2006). Theory of ferromagnetic (III,Mn)V semiconductor. *Rev. Mod. Phys.*, 78, 809–864, <https://doi.org/10.1103/RevModPhys.78.809>.
3. Dietl, T. (2002). Ferromagnetic semiconductors. *Semicon. Sci. Technol.*, 17, 377–380.
4. Zener, C. (1951). Interaction between the d shells in the transition metals. *Phys. Rev.*, 81, 440–444, <https://doi.org/10.1103/PhysRev.81.440>.
5. Anderson, P. W. & Hasegawa, H. (1955). Considerations on double exchange. *Phys. Rev.*, 100, 675–681, <https://doi.org/10.1103/PhysRev.100.675>.
6. Kanamori, J. & Terakura, K. (2001). A general mechanism underlying ferromagnetism in transition metal compounds. *J. Phys. Soc. Jpn.*, 70, 1433–1434, <https://doi.org/10.1143/JPSJ.70.1433>.
7. Kanamori, J. (1959). Superexchange interaction and symmetry properties of electron orbitals. *J. Phys. Chem. Solids*, 10, 87–98, [https://doi.org/10.1016/0022-3697\(59\)90061-7](https://doi.org/10.1016/0022-3697(59)90061-7).
8. Goodenough, J. B. (1955). Theory of the role of covalence in the perovskite-type manganites  $[La,M(II)]MnO_3$ . *Phys. Rev.*, 100, 564–673, <https://doi.org/10.1103/PhysRev.100.564>.

9. Moore, G. E. (1965). Cramming more components onto integrated circuits. *Electron.*, 38, 114–117.
10. Wolf, S. A. et al. (2001). Spintronics: A spin-based electronics vision for the future. *Sci.*, 294, 1488–1495, <https://doi.org/10.1126/science.1065389>.
11. Shiba, H. (1971). A reformulation of the coherent potential approximation and its applications. *Prog. Theory Phys.*, 46, 77–94, <https://doi.org/10.1143/PTP.46.77>.
12. Schmidt, G. et al. (2000). Fundamental obstacle for electrical spin injection from a ferromagnetic metal into a diffusive semiconductor. *Phys. Rev. B*, 62, R4790–R4796, <https://doi.org/10.1103/PhysRevB.62.R4790>.
13. Sato, K., Dederics, P. H. & Yoshida, H. K. (2003). Curie temperatures of III–V diluted magnetic semiconductors calculated from first-principles. *Europhys. Lett.*, 61, 403–408, <https://doi.org/10.1209/epl/i2003-00191-8>.
14. Dietl, T. et al. (2000). Zener model description of ferromagnetism in zinc-blende magnetic semiconductors. *Sci.*, 287, 1019–1022, <https://doi.org/10.1126/science.287.5455.1019>.
15. Kohn, W. & Rostoker, N. (1954). Solution of the schrödinger equation in periodic lattices with an application to metallic lithium. *Phys. Rev.*, 94, 1111–1120, <https://doi.org/10.1103/PhysRev.94.1111>.
16. Kohn, W. & Sham, L. J. (1965). Self-consistent equations including exchange and correlation effects. *Phys. Rev.*, 13, A1133–A1138, <https://doi.org/10.1103/PhysRev.140.A1133>.
17. Korringa, J. (1947). On the calculation of the energy of a bloch wave in a metal. *Phys.*, 13, 392–400, [https://doi.org/10.1016/0031-8914\(47\)90013-X](https://doi.org/10.1016/0031-8914(47)90013-X).
18. Perdew, J. P. (1986). Density-functional approximation for the correlation energy of the inhomogeneous electron gas. *Phys. Rev. B*, 33, 8822–8824, <https://doi.org/10.1103/PhysRevB.33.8822>.
19. Wyckoff, R. W. G. (1963). *Crystal structures*, 2nd ed. New York: Interscience Publishers.
20. Mašek, J., Kudrnovský, J. & Máca, F. (2003). Lattice constant in diluted magnetic semiconductors (Ga,Mn)As. *Phys. Rev. B*, 67, 153203–153206, <https://doi.org/10.1103/PhysRevB.67.153203>.
21. Akai, H. (2011). Ab-initio electronic structure calculation code. Retrieved 15 February 2018 from <http://kkriissp.u-tokyo.ac.jp>.
22. Shahjahan, M., Razzakul, I. M. & Rahman, M. M. (2016). First-principles calculation of stable magnetic state and curie temperature in transition metal doped III-V semiconductors. *Comput. Condens. Matt.*, 9, 67–71, <https://doi.org/10.1016/j.cocom.2016.10.001>.
23. Furdyna, J. K. (1988). Diluted magnetic semiconductors. *J. Appl. Phys.*, 64, R29–R64, <https://doi.org/10.1063/1.341700>.